Stu2 acts as a microtubule destabilizer in metaphase budding yeast spindles

Lauren Humphrey[a], Isabella Felzer-Kim[a,†], and Ajit P. Joglekar[a,b,*]
[a]Cell and Developmental Biology, University of Michigan Medical School, and [b]Department of Biophysics, University of Michigan, Ann Arbor, MI 48019

ABSTRACT **The microtubule-associated protein Stu2 (XMAP215) has the remarkable ability to act either as a polymerase or as a destabilizer of the microtubule plus end. In budding yeast, it is required for the dynamicity of spindle microtubules and also for kinetochore force generation. To understand how Stu2 contributes to these distinct activities, we analyzed the contributions of its functional domains to its localization and function. We find that Stu2 colocalizes with kinetochores using its TOG domains, which bind GTP-tubulin, a coiled-coil homodimerization domain, and a domain that interacts with plus-end interacting proteins. Stu2 localization is also promoted by phosphorylation at a putative CDK1 phosphorylation site located within its microtubule-binding basic patch. Surprisingly, however, we find that kinetochore force generation is uncorrelated with the amount of kinetochore-colocalized Stu2. These and other data imply that Stu2 colocalizes with kinetochores by recognizing growing microtubule plus ends within yeast kinetochores. We propose that Stu2 destabilizes these plus ends to indirectly contribute to the "catch-bond" activity of the kinetochores.**

Monitoring Editor
Thomas Surrey
The Francis Crick Institute

Received: Aug 4, 2017
Revised: Nov 15, 2017
Accepted: Nov 21, 2017

INTRODUCTION

Accurate segregation of chromosomes during cell division requires a stable attachment of sister kinetochores on each chromosome to microtubules emanating from opposite spindle poles. These kinetochore-microtubule attachments are termed "end-on" because the kinetochore binds to the tip of the microtubule plus end (McIntosh *et al.*, 2013). End-on kinetochore–microtubule attachments tightly couple chromosome movement to the growth and shrinkage of the microtubule plus ends. Such plus end–coupled movements of the chromosome and its bipolar attachment to the spindle result in its accurate segregation in anaphase.

The establishment and maintenance of end-on attachment requires the concerted action of several microtubule-binding kinetochore proteins, microtubule-associated proteins (MAPs), and motors. Individual contributions of these proteins are well understood in the case of the relatively simple kinetochore found in the budding yeast *Saccharomyces cerevisiae* (Malvezzi and Westermann, 2014). In budding yeast, the kinetochore initially interacts laterally with a microtubule lattice. The plus end–interacting protein (+TIP) Stu2/XMAP215 plays crucial but indirect roles in this process (Gandhi *et al.*, 2011; Vasileva *et al.*, 2017). These lateral interactions are transformed into end-on attachment to the plus end by the microtubule-binding activities of the Ndc80 complex, a highly conserved kinetochore component, and the yeast-specific Dam1 complex (Tanaka, 2010). In metaphase, an assembly of ~8 Ndc80 molecules and ~16–20 Dam1 complex molecules, which likely form an oligomeric ring, couples kinetochore movement with depolymerization at the plus end (Lampert *et al.*, 2010, 2013; Tien *et al.*, 2010; Aravamudhan *et al.*, 2014). Recent in vitro studies reveal that Stu2 is also essential for kinetochore force generation and for the "catch bond" behavior of yeast kinetochore particles, in which end-on attachment of the kinetochore to a depolymerizing microtubule tip becomes stronger in response to higher tension (Miller *et al.*, 2016).

The involvement of Stu2 in force generation is surprising, because it is primarily known as a regulator of microtubule polymerization dynamics. It polymerizes microtubule plus ends by acting as a tethered delivery system of tubulin dimers (Al-Bassam *et al.*, 2006;

This article was published online ahead of print in MBoC in Press (http://www.molbiolcell.org/cgi/doi/10.1091/mbc.E17-08-0494) on November 29, 2017.

†Present address: Department of Kinesiology, Michigan State University, East Lansing, MI 48824.

*Address correspondence to: Ajit P. Joglekar (ajitj@umich.edu).

Abbreviations used: CDK1, cyclin-dependent kinase 1; FRAP, fluorescence recovery after photobleaching; GFP, green fluorescent protein; HU, hydroxy urea; MAP, microtubule-associated protein; ORF, open reading frame; +TIP, Plus Tip-Interacting Protein; TOG, tumor overexpressed gene; UTR, untranslated region; YPD, yeast extract, peptone, dextrose.

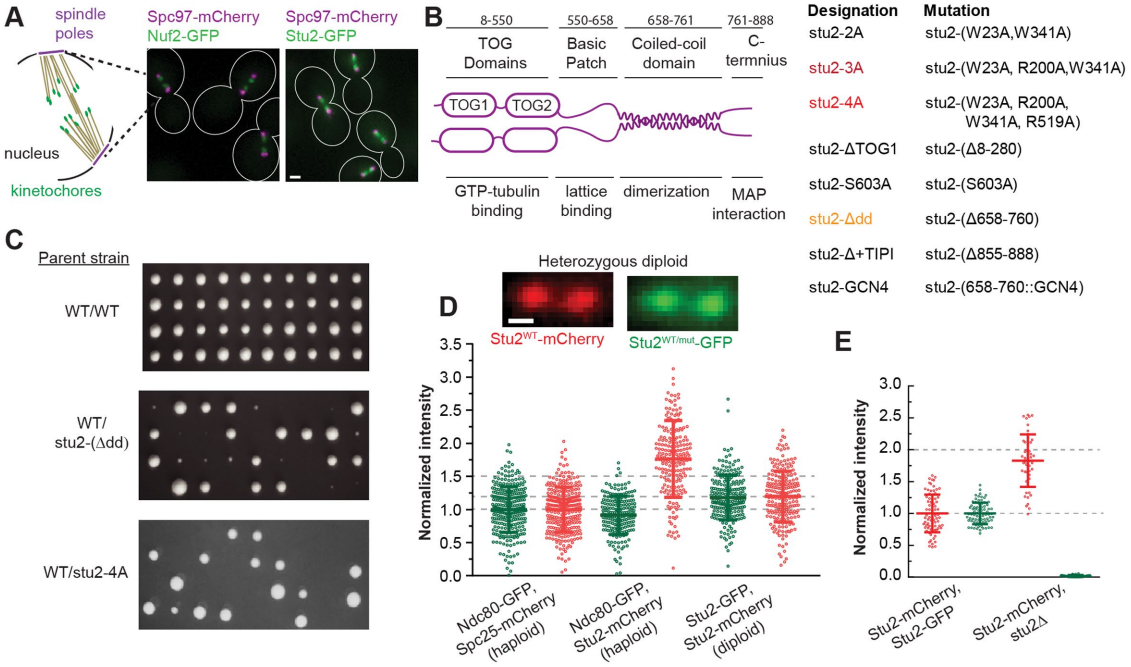

FIGURE 1: Functional domains of Stu2. (A) Cartoon of the intranuclear spindle in budding yeast. Micrographs on the right reveal the colocalization of bioriented kinetochore clusters (visualized by Nuf2-GFP) and Stu2 in metaphase-arrested cells. Spindle poles visualized by Spc97-mCherry. Note that individual yeast kinetochores cannot be resolved due to the large number of kinetochores (16 sister kinetochore pairs) and the small size of the spindle (~1.7 µm on average, scale bar ~0.5 µm). (B) Left: organization of the functional domains in Stu2 and their known biochemical activities. Amino acid positions are indicated by the numbers above. Right: list of mutant alleles of Stu2 studied and the designations used. Lethal mutations are highlighted by red letters; deleterious mutations are highlighted by orange letters. (C) Tetrad analysis of heterozygous diploid yeast strains carrying a wild-type and a mutant allele of STU2 (each column of four yeast colonies is produced by the four spores of a meiotic event). (D) Top: colocalization of Stu2-GFP and Stu2-mCherry in a heterozygous diploid yeast strain. Scatterplot: comparison of normalized fluorescence signals from metaphase kinetochore clusters in the indicated strains. Note that Stu2 is ~1.5-fold more abundant than the Ndc80 complex. In the heterozygous diploid strain expressing Stu2-GFP and Stu2-mCherry, the amount of each allele is ~1.2-fold higher than that of the Ndc80 complex ($n = 208$, 222 from two repeats and 308 from three repeats, respectively) scale bar ~0.5 µm. (E) Normalization scheme used to compare wild-type (Stu2-mCherry) and mutant (stu2Δ in this case) protein. Notice that Stu2-mCherry compensates for the loss of localization due to the mutation. ($n = 78$ from four repeats and $n = 75$ from three repeats.)

Brouhard *et al.*, 2008; Ayaz *et al.*, 2012). Equally surprising is the observation that Stu2 destabilizes microtubules in mitotic yeast cells (Kosco *et al.*, 2001; van Breugel *et al.*, 2003). However, the mechanisms by which Stu2 contributes to kinetochore force generation or to the dynamicity of spindle microtubules remain unknown. For either function, Stu2 must localize in the kinetochore near the plus end of the microtubule. Indeed, the centroid of fluorophore-labeled Stu2 molecules coincides with the expected position of microtubule plus ends within bioriented kinetochores (which themselves appear as two puncta, each containing 16 kinetochores in metaphase; see Figure 1A; McIntosh *et al.*, 2013; Aravamudhan *et al.*, 2014). Importantly, this Stu2 localization is dynamic: Stu2 molecules turn over completely at a rate that is twice as high as the rate of tubulin turnover (Maddox *et al.*, 2000; Aravamudhan *et al.*, 2014). Thus, Stu2 is in a position to contribute to kinetochore movement either directly, by generating force, or indirectly, by acting on the plus end, or via both activities.

To elucidate how Stu2 contributes to kinetochore motility, we systematically analyzed the contributions of individual functional domains in Stu2 to its colocalization with bioriented kinetochores in budding yeast. Surprisingly, we found that Stu2 localization arises out of distinct contributions from disparate biochemical activities rather than a specific protein–protein interaction. Of these activities, the ability of Stu2 to recognize and bind to GTP-tubulin is essential. Its localization is further enhanced by mitosis-specific phosphorylation at a conserved CDK1 site in the basic patch of Stu2. We also find that Stu2 is dispensable after yeast kinetochores establish bipolar attachments. Using these observations, we propose that Stu2-mediated plus-end destabilization counteracts the tension-dependent rescue of the plus end by the Ndc80-Dam1 assembly. This in turn ensures that the Ndc80-Dam1 assembly consistently interacts with the depolymerizing plus end to withstand tension and gives rise to the "catch-bond" behavior.

RESULTS AND DISCUSSION

As a regulator of microtubule dynamics, Stu2 performs several distinct functions during mitosis. It promotes microtubule polymerization to facilitate the capture of unattached kinetochores. It is required for the "catch-bond" activity of bioriented yeast kinetochores (Tanaka *et al.*, 2007; Miller *et al.*, 2016; Vasileva *et al.*, 2017). It also promotes microtubule turnover during metaphase (Kosco *et al.*, 2001; van Breugel *et al.*, 2003; Wolyniak *et al.*, 2006). Finally, Stu2 is implicated in driving spindle elongation in anaphase B (Severin *et al.*, 2001). Therefore, to understand how Stu2 contributes specifically to the catch-bond activity of yeast kinetochores under tension,

that is, bioriented kinetochores, we first sought to determine how Stu2 interacts with the kinetochore under this condition.

Early studies of Stu2 describe it as a microtubule-associated protein (He *et al.*, 2001; Kosco *et al.*, 2001). However, we have previously shown that Stu2 colocalizes to a large degree with bioriented kinetochores. In metaphase-arrested cells, Stu2 localization is distinct from the localization of the plus-tip interacting proteins (+TIPs) Bim1/EB1, which is distributed along the entire length of the spindle, and Bik1/CLIP-170, which is skewed toward the spindle poles (Supplemental Figure S1A; Aravamudhan *et al.*, 2014). Although we arrested cells in metaphase using conditional repression of *CDC20* in these experiments, this treatment does not detectably alter either the amount of tubulin polymer or its distribution in the mitotic spindle (Supplemental Figure S1B). In fact, the spatial distribution of Stu2 molecules over the length of the metaphase spindle is identical to the distribution of the Dam1 complex (Supplemental Figure S1C). It is likely that a fraction of the Stu2 molecules are microtubule-associated, given that Stu2 interacts with Bim1 and Bik1 and kinesin motors (Wolyniak *et al.*, 2006; Gandhi *et al.*, 2011; Vasileva *et al.*, 2017). However, because of the ~250-nm average length of the kinetochore-attached microtubules, optical microscopy cannot individually resolve the kinetochore-localized and microtubule-associated populations of Stu2 molecules.

To elucidate the molecular basis of Stu2 interaction with metaphase kinetochores, we determined the individual contributions of its five functional domains to achieving its metaphase localization (Figure 1B, left; Al-Bassam *et al.*, 2006). In its N-terminal half, Stu2 contains two TOG domains, TOG1 and TOG2, which bind to GTP-tubulin present either in solution or in the form of the GTP cap on a polymerizing microtubule plus end (Ayaz *et al.*, 2012). The TOG domains are followed by an unstructured domain containing many basic residues. This "basic patch" interacts electrostatically with the acidic tails, or "E-hooks," of tubulin. The basic patch leads into an extended coiled-coil domain that mediates Stu2 homodimerization. Finally, the C-terminal domain of Stu2 interacts with Bim1 and Bik1 (Wolyniak *et al.*, 2006). To dissect the contributions of these domains to Stu2 localization in metaphase, we used gene replacement to introduce Stu2 mutations that abrogate the activity of individual domains (Figure 1B, right; *Materials and Methods*).

A subset of the mutations in Stu2 either severely reduced or abolished the viability of haploid yeast strains (photographs in Figure 1C; Supplemental Figure S2A; also highlighted in the table in Figure 1B). Therefore, to study the localization phenotypes of such lethal mutations, we adopted an alternative strategy (Figure 1D). We examined the colocalization of mutant and wild-type alleles of Stu2 in heterozygous diploid strains, wherein the wild-type *STU2* is tagged at its C-terminus with mCherry and the mutant allele is tagged similarly with GFP. These heterozygous diploid strains are viable. Furthermore, gene replacement ensured that the expression of the mutant protein was similar to that of the wild-type protein (Supplemental Figure S3A). Therefore, this strategy enabled the quantification and comparison of the abilities of the mutant and wild-type Stu2 to localize to the spindle in the same cell.

One drawback of this strategy is that the mutant protein can dimerize with wild-type Stu2, which will partially mask the effects of the mutation. Therefore, the observed phenotypes of the mutation are expected to be less severe than the true phenotypes. Consistent with this expectation, the heterozygous strains did not exhibit detectable defects in microtubule attachment as judged by their ability to grow on media containing low doses of the microtubule-destabilizing drug benomyl (Supplemental Figure S2B). We also did not detect any defects in the timing of the metaphase-to-anaphase transition (Supplemental Figure S2C).

To assess the impact of the selected Stu2 mutations on its metaphase localization, we first verified that wild-type Stu2-GFP and wild-type Stu2-mCherry colocalize in similar quantities in heterozygous diploid strains. In these and subsequent experiments, we imaged cells from mid–log phase cultures and analyzed only those cells wherein two distinct clusters of bioriented kinetochores were visible. We refer to the kinetochores in these clusters as metaphase kinetochores. The GFP and mCherry fluorescence signals from a cluster of bioriented kinetochores cannot be directly compared, because the fluorescence depends not only on protein counts but also on the brightness of the two fluorophores and the excitation intensity used for each. Therefore, to normalize and compare the two signals, we used the respective signals of Ndc80-GFP and Spc25-mCherry expressed in a haploid strain. GFP and mCherry fluorescence signals from a kinetochore cluster in this strain corresponds to the same number of molecules, because the composition of the Ndc80 complex dictates a 1:1 of GFP to mCherry stoichiometry. Normalization of Stu2-GFP and Stu2-mCherry fluorescence signals with Ndc80-GFP and Spc25-mCherry, respectively, confirmed that the two Stu2 alleles colocalize with kinetochores in equal quantities (Figure 1D). We used the Stu2-GFP and Stu2-mCherry intensities in this wild-type diploid strain to normalize the respective signals measured in other heterozygous diploid strains, so that the ability of the wild-type and mutant Stu2 proteins to localize to metaphase kinetochores can be quantified (Figure 1E).

In metaphase cells, Stu2 dynamically localizes in the close vicinity of the plus ends of kinetochore microtubules (Aravamudhan *et al.*, 2014). The TOG domains of Stu2 recognize GTP-tubulin at the plus ends of polymerizing microtubules in vitro (van Breugel *et al.*, 2003; Ayaz *et al.*, 2012; Maurer *et al.*, 2014). Therefore, we first tested the hypothesis that the TOG domains colocalize Stu2 with metaphase kinetochore clusters. When we introduced progressively severe mutations in the TOG domains to impair their ability to bind to GTP-tubulin, the localization of the mutant Stu2 diminished progressively (Figure 2A). Interestingly, the loss of the mutant protein was compensated for by a corresponding increase in the wild-type Stu2-mCherry. Abrogation of the GTP-tubulin-binding activity of both TOG domains significantly reduced Stu2 localization and also led to lethality in haploid strains (Figure 1B; Supplemental Figure S2A). The strong correlation between the ability of the TOG domains to recognize and bind specifically to GTP-tubulin and Stu2 localization reveals that the TOG domains play a crucial role in colocalizing Stu2 with kinetochores in metaphase. The TOG domains are unlikely to interface directly with kinetochore subunits, given that they detect the shape and curvature of the GTP-tubulin dimer (Ayaz *et al.*, 2012).

We next studied the contribution of the basic patch in Stu2 to its localization. Electrostatic interactions between the basic patch and tubulin E-hooks should distribute Stu2 evenly along the entire lattice of spindle microtubules. However, Stu2 is mostly concentrated near the plus ends of kinetochore-bound microtubules (Figure 1A). To reconcile the Stu2 distribution predicted by the activity of the basic patch with the observed localization, we hypothesized that the net positive charge of the basic patch may be neutralized by mitosis-specific phosphorylation at a putative CDK1 phosphorylation site located within the basic patch (Aoki *et al.*, 2006). To test this hypothesis, we examined the localization of stu2-S603A, a Stu2 allele that cannot be phosphorylated at the CDK1 phosphorylation site (Figure 2B). Unlike wild-type Stu2, stu2-603A localized uniformly over the entire spindle. Examination of stu2-S603A along cytoplasmic microtubules indicated that the spindle localization was due to the

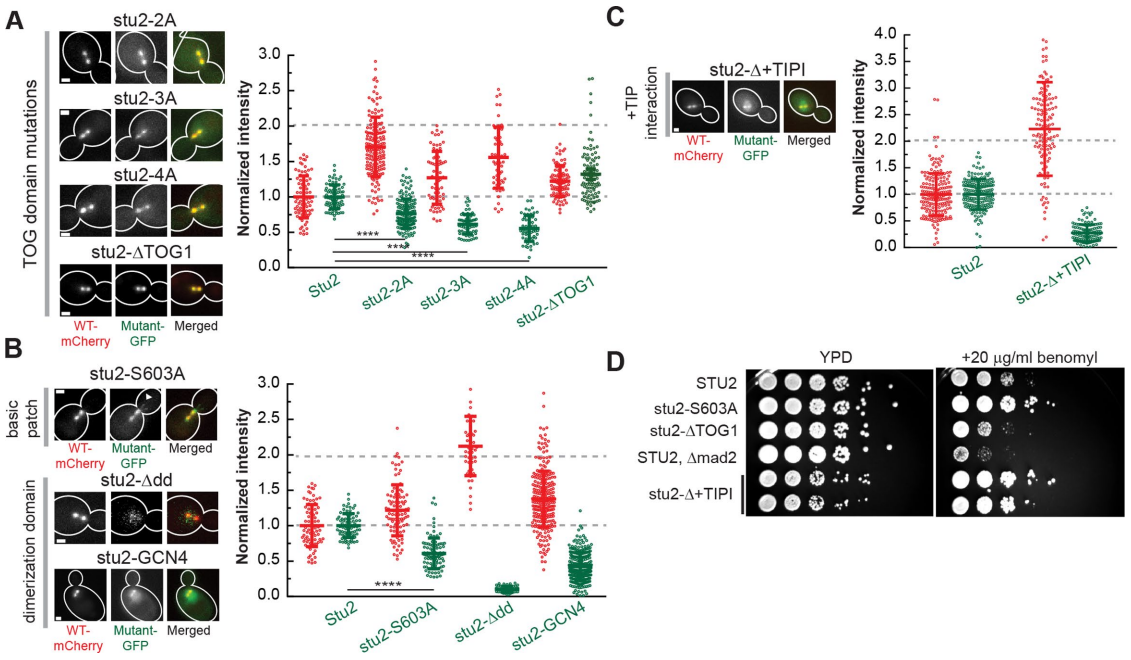

FIGURE 2: The contribution of functional domains in Stu2 to its metaphase localization. (A) Effects of mutations in the GTP-binding TOG domains. Left: representative micrographs of heterozygous diploid yeast strains expressing mCherry-tagged wild-type Stu2 and GFP-tagged mutant Stu2 (mutations indicated at the top of each micrograph panel). Right: normalized intensity scatterplots for the mutations displayed. Horizontal lines display mean ± SD. (n = 78, 162, 68, 54, 101 from two or three experiments.) Scale bar ~1 μm. (B) Contributions of the basic patch and the dimerization domain (n = 78, 99, 86, 272, respectively, from >2 experiments). Scale bar ~1 μm. (Asterisks in A and B indicate statistical significance obtained from a nonparametric Mann–Whitney test.) (C) Effects of the deletion of the +TIP interaction domain of Stu2 (n = 196, 134 for wild type and stu2-Δ+TIPI, respectively, from two experiments). Scale bar ~1 μm. (D) Benomyl sensitivity of haploid strains carrying the indicated mutations in Stu2. *mad2*Δ, which cannot survive on benomyl-containing media, was used as the negative control (representative photograph shown, plating performed twice).

binding of the mutant protein along the entire microtubule lattice (Figure 2B, white arrowheads; also see additional examples and quantitative analysis of protein distribution provided in Supplemental Figure S3, B and C). The dispersed distribution also decreased the level of kinetochore-colocalized stu2-S603A (Supplemental Figure S3C). Localization of the nonphosphorylatable Stu2 is consistent with the expected activity of the basic patch. Conversely, neutralization of the basic patch via phosphorylation will significantly reduce its binding to the microtubule lattice and thereby enable other Stu2 domains to concentrate the protein near the plus end.

The dimerization domain in Stu2 is not expected to be important for microtubule binding. Therefore, we studied the phenotype of a previously designed allele of Stu2, stu2-Δdd, wherein this domain is deleted (Al-Bassam *et al.*, 2006). Strikingly, stu2-Δdd was unable to localize to the spindle in heterozygous diploid cells (Figure 2B). The cellular level of stu2-Δdd was ~50% lower than expected, but this decrease does not fully explain the drastic loss in its localization (Supplemental Figure S3A). The delocalization of stu2-Δdd is surprising because it retains all of its microtubule-binding activities (Al-Bassam *et al.*, 2006). Interestingly, stu2-ΔTOG1, wherein the first TOG domain is deleted, fully retained its metaphase localization even though this allele contains the same number of TOG domains as stu2-Δdd (Figure 2A; Supplemental Figure S3D). Therefore, we conclude that the stereotypical metaphase localization of Stu2 requires a minimum of two dimerized TOG domains.

The observed loss of Stu2 localization could also be due to the removal of an unanticipated kinetochore-interacting motif located in the dimerization domain. To test this possibility, we replaced the dimerization domain with an artificial coiled-coil dimerization domain in the form of the much shorter Leucine Zipper (GCN4). It should be noted that this engineered Stu2 protein is unlikely to heterodimerize with wild-type Stu2. Strikingly, artificially homodimerized stu2-GCN4 regained its kinetochore localization, although its abundance was ~50% lower than that of wild-type Stu2 (Figure 2B). The mutant allele also restored the viability of haploid yeast strains (Supplemental Figure S3E). Moreover, despite the ~50% reduction in kinetochore-colocalized stu2-GCN4, kinetochore force generation remained unaffected (Supplemental Figure S3G).

Finally, we investigated the role of the +TIP-interaction (+TIPI) domain of Stu2 by replacing it with GFP (stu2-Δ+TIPI; Figure 2C). In heterozygous diploid cells stu2-Δ+TIPI localized within kinetochore clusters, but its abundance was significantly reduced. Despite this reduction, haploid yeast strains carrying stu2-Δ+TIPI were viable (Figure 2D). Therefore, we quantified the colocalization of stu2-Δ+TIPI with Ndc80-mCherry in a haploid strain. Consistent with the results from heterozygous diploid cells, stu2-Δ+TIPI colocalized with Ndc80, although at significantly reduced levels (Supplemental Figure S3, D, right, and G, left). The mutation also did not detectably affect the separation between bioriented sister kinetochores, suggesting that kinetochore force generation was unaffected (Supplemental Figure S3G, right).

The systematic analysis of each functional domain in Stu2 offers a key insight into the mechanism of Stu2 localization. It reveals that

all Stu2 domains contribute to its colocalization with bioriented kinetochores. Thus, Stu2 localization emerges out of complex interactions rather than a specific protein–protein interaction between Stu2 and a kinetochore subunit. The necessity of homodimerized TOG domains for Stu2 localization is striking, because neither the TOG domains nor the homodimerization domain harbor kinetochore-interaction motifs. Therefore, the ability of Stu2 to bind GTP-tubulin specifically appears to be crucial for colocalizing Stu2 with metaphase kinetochores. This observation implies that Stu2 binds transiently to GTP-tubulin in polymerizing plus ends embedded in the kinetochore. Consistent with this notion, Stu2 turns over at a rate that is twice as high as the rate of tubulin turnover in metaphase (Aravamudhan *et al*., 2014). The absence of a specific protein–protein interaction in mediating Stu2 localization and its rapid turnover are both markedly different from the properties of the Dam1 complex, another MAP and the bona fide force generator of the yeast kinetochore. Dam1 is stably associated with the yeast kinetochore in metaphase and its localization is mediated by a specific protein–protein interaction (Joglekar *et al*., 2006; Lampert *et al*., 2013; Kim *et al*., 2017). It is possible that there are two colocalized, but distinct, Stu2 populations: one that transiently binds GTP-tubulin in growing microtubule plus end and the other stably bound to the kinetochore. However, the presence of a stable Stu2 population is unlikely because the kinetochore-colocalized Stu2 turns over completely, as revealed by fluorescence recovery after photobleaching (FRAP) experiments (the convergence of the curves displaying fluorescence recovery in the bleached cluster and the loss of fluorescence in the unbleached cluster in Supplemental Figure S4A indicate that fluorescence recovery is only limited by the availability of unbleached fluorophores; also see Aravamudhan *et al*., 2014).

The mitosis-specific phosphorylation in the basic patch of Stu2 offers a key insight into Stu2 function. The microtubule-binding activity of the basic patch of XMAP215 is required for its polymerase activity (Widlund *et al*., 2011). If the basic patch is similarly required for Stu2 polymerase activity, then its negation via phosphorylation will also impair the polymerase activity by neutralizing its ability to bind to the microtubule lattice. To test this idea, we observed the growth of haploid yeast strains carrying nonlethal mutations in Stu2 on media containing benomyl (Figure 2D). We reasoned that mutations that decrease Stu2 polymerase activity would be unsuitable for survival under conditions where microtubules are abnormally unstable (e.g., in media containing a low dose of benomyl). Consistent with this reasoning, deletion of the first TOG domain in Stu2 (stu2-ΔTOG1), which reduces the polymerase activity, adversely affected colony growth on benomyl-containing media (Figure 2D). Conversely, Stu2 mutations that enhance its polymerase activity should counteract the effects of benomyl and enable more robust colony growth. Indeed, a haploid strain expressing stu2-S603A grew markedly better than wild-type cells on the benomyl-containing media. This observation is consistent with the notion that the basic patch contributes to Stu2 polymerase activity by enhancing its tethering near the plus end (Ayaz *et al*., 2014). Our observation, when considered together with the requirement of Stu2 for dynamic microtubules (Kosco *et al*., 2001; Wolyniak *et al*., 2006) and the finding that Stu2 is a microtubule plus-end destabilizer (van Breugel *et al*., 2003), suggests that mitosis-specific phosphorylation within the basic patch transforms Stu2 from a plus-end polymerase into a destabilizer.

Interestingly, strains carrying stu2-Δ+TIPI grew more robustly on benomyl-containing media than all other strains, even though the stu2-Δ+TIPI mutation resulted in significantly slower growth on normal media (Figure 2D). Thus, even though stu2-Δ+TIPI colocalizes with kinetochores in a significantly lower amount, it enables robust growth of yeast cells on benomyl-containing media. In contrast, stu2-ΔTOG1 colocalizes with kinetochore clusters as well as wild-type Stu2, but it does not support the growth of yeast cells under the same conditions (Figure 2, A and D). This striking observation suggests that the deletion of the +TIP interacting domain may impact Stu2 functions unrelated to Stu2 activity in metaphase kinetochores.

Because all five functional domains of Stu2 contribute to its characteristic colocalization with metaphase kinetochores, we could not design a separation of function mutation that selectively abrogates kinetochore interaction. Therefore, we had to resort to the conditional delocalization strategy based on the "Anchor Away" technique in order to elucidate Stu2 function before and after kinetochore biorientation (*Materials and Methods*; Haruki *et al*., 2008). We tagged Stu2 with Frb-GFP and Tub4, a spindle pole body component chosen because of its high copy number, with Fkbp12 (Figure 3A). When metaphase-arrested cells were treated with rapamycin, Stu2-Frb-GFP strongly dimerized with Tub4-Fkbp12. This resulted in ~70% depletion of Stu2 from the kinetochore clusters, leaving only ~2 Stu2 dimers on average per kinetochore (Supplemental Figure S4E). The delocalized protein was stably anchored at the spindle pole bodies as evidenced by the lack of detectable FRAP (Supplemental Figure S4B). Surprisingly, the significant Stu2 depletion had no detectable effect on the bioriented sister kinetochores (Figure 3C). The length of the metaphase spindle also remained unaffected (Figure 3D). These observations demonstrate that even after significant reduction in Stu2 colocalized with kinetochores, the steady-state distribution of kinetochores in metaphase and the balance of opposing forces that maintains a constant spindle length remain unaffected. In agreement with previous observations (Severin *et al*., 2001), the depletion of free Stu2 from the spindle also reduced the rate of spindle elongation during anaphase B (Supplemental Figure S4C).

We next used the "Anchor Away" strategy to assess specifically the functional significance of the dynamic Stu2 localization, without perturbing the position with respect to kinetochores. For this, we dimerized Stu2 with the C-terminus of Spc24, which is located at the centromeric end of the Ndc80 complex (Figure 3, E and F). We first observed the effect of suppressed Stu2 turnover on the formation of bipolar spindles. We anchored Stu2 to the C-terminus of Spc24 in G1-arrested cells, released them into the cell cycle, and then experimentally prevented the cells from entering anaphase. As expected, a majority of untreated cells achieved kinetochore biorientation in 30–60 min (Figure 3G). In contrast, rapamycin-treated cells experienced significant delays in forming metaphase spindles, even though Stu2 was statically localized in the close vicinity of its normal, dynamic localization (Figure 3G, bar graph; it should be noted that short-term rapamycin treatment does not have any detectable effects on cell cycle progression; Supplemental Figure S4F). The observed effects could arise from a combination of two causes. First, Stu2 plays a key role in the establishment of lateral kinetochore-microtubule interaction and its conversion into end-on attachment (Gandhi *et al*., 2011; Vasileva *et al*., 2017). Moreover, Stu2-mediated microtubule turnover may also be essential for kinetochore biorientation (Bakhoum *et al*., 2009). We also cannot rule out the possibility that defects in Stu2 conformation relative to the plus end induced by rapamycin-induced dimerization of Stu2-Frb with Spc24-2xFkbp12, or inadvertent impairment of Ndc80 function due to the dimerization, contribute to the observed phenotype.

We also assessed Stu2 function in anaphase progression. In this experiment, we suppressed Stu2 turnover in metaphase-arrested

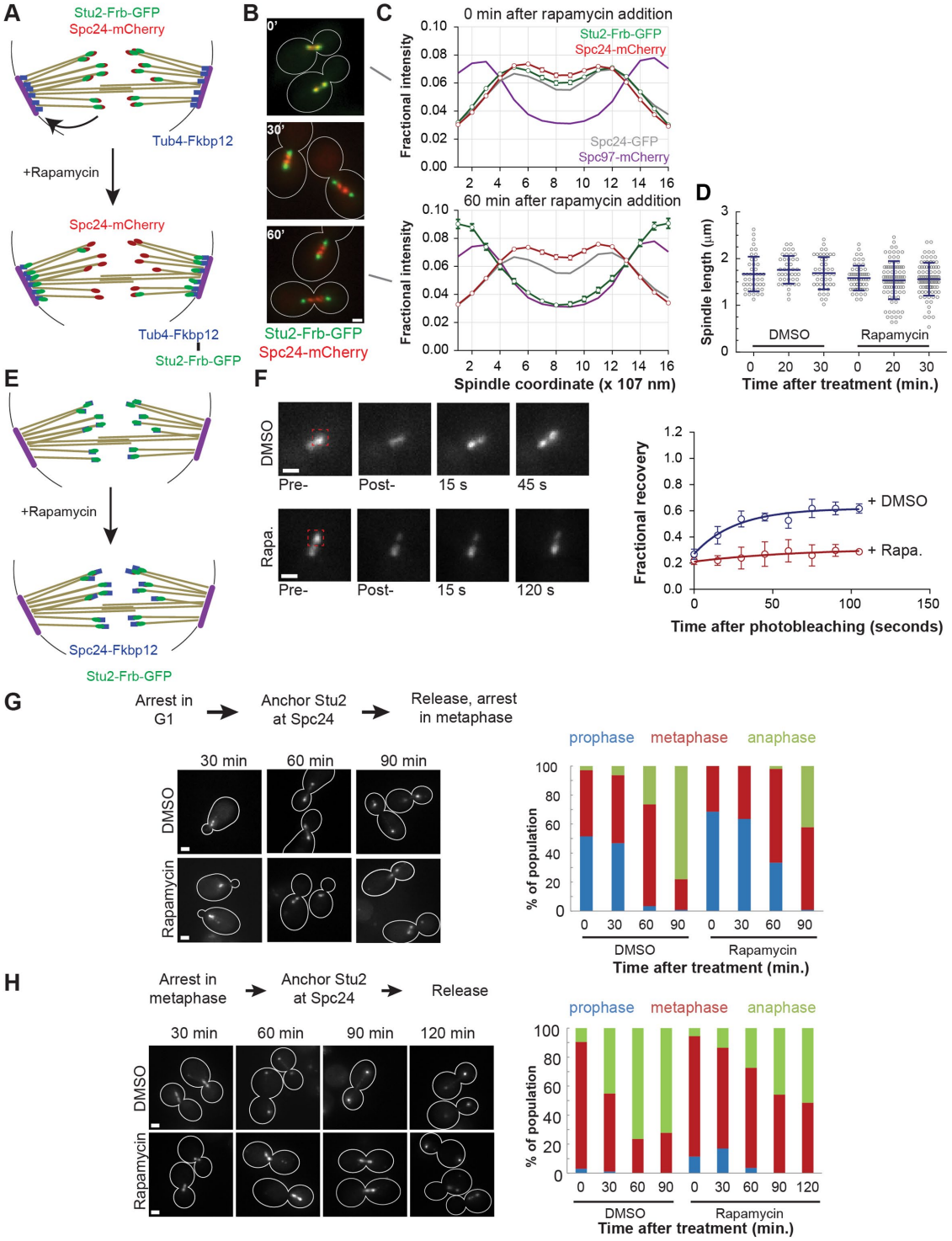

FIGURE 3: Effects of conditional mislocalization and conditional suppression of the turnover of Stu2. (A) Cartoon schematic for the expected effect of rapamycin treatment on Stu2-Frb-GFP localization with Tub4-FKBP. (B) Fluorescence micrographs show Stu2-Frb-GFP and kinetochore (Spc24-mCherry) localization in metaphase-arrested cells before and after the addition of rapamycin to culture media, thus anchoring Stu2 to Tub4-FKBP. Number in the top left corner indicates the time after rapamycin addition. Scale bar ~1 μm. (C) Normalized intensity distribution along the spindle axis for the indicated fluorescently labeled proteins. Line scans from a strain expressing Spc24-GFP (kinetochore protein) and Spc97-mCherry (spindle pole body protein) are overlaid for reference. 0 min: Stu2/Spc24 $n = 84$ three repeats, 60 min: Stu2/Spc24 $n = 89$ three repeats. Both: Spc97 control $n = 56$ one repeat, Spc24 control $n = 12$ one repeat. (D) The effect of Stu2 mislocalization on the spindle length in metaphase-arrested cells. (For each column, left to right: $n = 45, 64, 42, 58, 93, 88$, respectively; horizontal lines display mean ± std. dev.) (E) Cartoon depicts the scheme used to suppress Stu2 turnover, while maintaining its metaphase localization. (F) Fluorescence recovery after photobleaching quantifies the effect of rapamycin on Stu2 turnover (DMSO $n = 10$, rapamycin $n = 11$ cells, mean

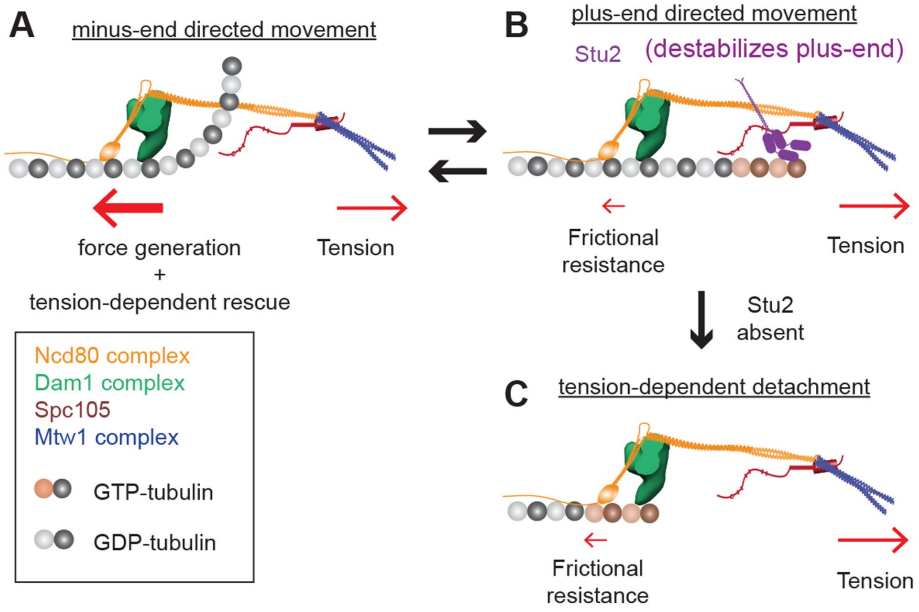

FIGURE 4: Proposed role of Stu2 in the catch-bond activity of yeast kinetochores. (A) When attached to a depolymerizing microtubule tip, the kinetochore uses the Ndc80-Dam1 assembly to generate depolymerization-coupled movement even against high opposing forces, or tension. The Dam1 ring also produces tension-dependent rescue. (B) When the microtubule tip is polymerizing, however, the Ndc80-Dam1 assembly can only offer a weak, frictional resistance to tension. Under this condition, the plus-end destabilizing activity of Stu2 ensures that the Ndc80-Dam1 assembly is able to reengage the depolymerizing microtubule tip and oppose high tension. This tension-dependent behavior leads to the catch-bond property of yeast kinetochore particles. (C) If Stu2 is depleted, the imposed tension will drag the kinetochore off the plus end.

cells and then released the cells into anaphase (Figure 3H). As expected, majority of the untreated cells completed anaphase by ~30 min. In contrast, rapamycin-treated cells were significantly delayed. Again, there are two possible mechanisms by which Stu2 contributes to anaphase progress. Stu2 may facilitate microtubule-depolymerization coupled movement and in anaphase it may act as a microtubule polymerase on the interpolar microtubules to enable spindle elongation (Severin *et al.*, 2001; Miller *et al.*, 2016). These observations further indicate that Stu2 is not directly involved in kinetochore force generation.

To reconcile the microtubule destabilizing activity of Stu2 observed in vivo with its essential role in force generation inferred from in vitro force clamp experiments, we propose the following model (Figure 4). Extensive in vitro studies reveal that the assembly of Ndc80 and Dam1 ring complex generates a minus end–directed movement coupled to microtubule depolymerization (Figure 4A; Asbury *et al.*, 2006; Powers *et al.*, 2009; Lampert *et al.*, 2010; Tien *et al.*, 2010). When interacting with a depolymerizing microtubule tip, the Dam1 ring harnesses the energy released by the outward curling of depolymerizing tubulin protofilaments to withstand a large plus end–directed force (Grishchuk *et al.*, 2008; Volkov *et al.*, 2013). The opposition to depolymerization offered by the Dam1 ring also induces tension-dependent rescue of the plus end: High tension makes the switch from depolymerization to polymerization more likely (Franck *et al.*, 2007; Akiyoshi *et al.*, 2010; Miller *et al.*, 2016). Importantly, after such a tension-dependent rescue, the Ndc80-Dam1 assembly must maintain its attachment with a growing plus end even as the tension pulling the kinetochore toward the plus end persists (Figure 4B). However, with the plus end now polymerizing, the Ndc80-Dam1 assembly can only offer frictional resistance of less than 1 pN (Akiyoshi *et al.*, 2010; Miller *et al.*, 2016). The likely outcome of this force imbalance is the detachment of the Ndc80-Dam1 assembly from the plus end with a probability of detachment that is proportional to the magnitude of the applied tension (Figure 4C) (Miller *et al.*, 2016). If Stu2 is present in this experiment, it will destabilize the growing plus end and enable the Ndc80-Dam1 assembly to reengage the now depolymerizing plus end and generate minus end–directed force opposing the applied tension (Aravamudhan *et al.*, 2014). Thus, Stu2 will play an indirect role in realizing the "catch-bond" activity of yeast kinetochore particles. This model explains why both Stu2 and Dam1 are essential for force generation, even though the Dam1 ring alone can suffice for generating the same magnitude of force (Volkov *et al.*, 2013; Umbreit *et al.*, 2014).

Although our model reconciles the in vivo Stu2 activity with in vitro data, further investigations are necessary to test it in vivo for two reasons. First, the model predicts that depletion of Stu2 should result in tension-dependent detachment of the kinetochore. However, we did not observe this in our Stu2 delocalization experiments (Figure 3). Similar observations were also made by a previous study, which found that sister kinetochore separation in metaphase yeast cells is unaffected even when microtubule turnover is suppressed by low doses of benomyl without affecting Stu2 directly (Pearson *et al.*, 2003). The lack of kinetochore detachment suggests that centromeric tension rarely exceeds 4–5 pN, a tension range that kinetochore–microtubule attachments can withstand for tens of minutes (Akiyoshi *et al.*, 2010). Second, it also remains to be seen whether the load-bearing characteristics of the yeast kinetochore derived from observations of its in vitro interaction with mammalian microtubules are the same as its load-bearing characteristics in vivo (Akiyoshi *et al.*, 2010; Miller *et al.*, 2016). Recent studies show that the parameters characterizing dynamic instability for yeast and vertebrate tubulin are

± SEM.) Scale bar ~1 µm. (G, H) Effects of suppressed Stu2 turnover on kinetochore biorientation (G) and on anaphase onset (H). The experimental scheme is noted at top left in each panel. Representative micrographs at selected time points shown at bottom left. Cells at each time point were scored using the following morphological criteria. Prophase cells: cells with only a single kinetochore cluster (visualized by the kinetochore-anchored Stu2-Frb-GFP). Metaphase cells: mitotic yeast cells with two clearly separated kinetochore clusters. Anaphase cells: large budded cells with kinetochore clusters separated by >4 µm. Bar graphs in each panel display the quantification obtained by combining scoring results from three independent experiments. (In G left to right: $n = 68, 128, 439, 246, 54, 159, 252, 358$, respectively. In H left to right: $n = 620, 537, 263, 180, 592, 464, 582, 392, 200$, respectively.) Scale bar ~1.5 µm.

significantly different and that MAPs can have distinctly different interactions with the two tubulins (Podolski *et al.*, 2014; Driver *et al.*, 2017). These differences are likely to affect transitions of the kinetochore-attached plus end between polymerization and depolymerization and the coupling of kinetochore movement through these transitions. Quantitative in vitro and in vivo measurements of the biophysical properties of yeast kinetochores are essential to fully understand their catch-bond activity and the role that Stu2 plays in realizing this activity.

MATERIALS AND METHODS

Strain construction

Yeast strains were transformed with PCR amplified GFP-fusion cassettes as described previously (Longtine *et al.*, 1998). Gene replacement was achieved via homology-directed integration of a linear DNA fragment consisting of STU2 promoter (1014 base pairs upstream of START), the STU2 ORF fused with GFP ORF followed by the G418 resistance gene, and ending in the STU2 3′ UTR (283 base pairs downstream from STOP) in a yeast strain hemizygous for STU2. This fragment was cloned into the pRS305 vector using *Sac*II and *Apa*I sites.

Yeast culture and imaging conditions

Cells were grown in yeast nitrogen base and dextrose (synthetic media) medium or grown in yeast extract, peptone, and dextrose (YPD) medium at 32°C and imaged at room temperature. Before imaging, cells were washed once with synthetic media and then immobilized on coverslips coated with concanavalin A. To synchronize cells in G1, α-factor was added at 2 μg/ml for 90 min and supplemented again for an additional 30 min. To image cell cycle progression, the α-factor was washed out, and cells were transferred to YPD media. To image metaphase-arrested cells, cells were first grown in synthetic media lacking methionine for 1 h and then transferred to media containing 2.75 mM methionine (Fisher Scientific BP388-100) for 2.5 h. To image the release from the metaphase arrest, these cells were then washed into methionine-free media. In experiments involving the "Anchor Away" technique, rapamycin (Fisher Scientific NC9362949) was added to a final concentration 1 μg/ml in the imaging culture. Dimethyl sulfoxide (DMSO) (Fisher Scientific BP231-100; 1 μg/ml imaging culture) was used as the vehicle control. To observe timing of the metaphase-anaphase transition, cells were synchronized in S phase by treating with 100 mM hydroxyurea (HU; Sigma-Aldrich H8627) for 2.5 h. HU was washed out before imaging.

Image acquisition and analysis

We used a Nikon Ti-E inverted microscope with a 1.4 NA, 100× oil immersion objective. The 1.5× tube lens was also used when necessary. Images were acquired on an Andor EMCCD camera (iXon 3) using MetaMorph acquisition software. A Lumencor LED light engine was used for fluorophore excitation. For each experiment, a 10-plane Z-stack was acquired with a separation of 200 nm between adjacent planes for a field of cells. The total fluorescence from each cluster of proteins tagged with either GFP or mCherry was measured using ImageJ or a custom MatLab program as previously described (Aravamudhan *et al.*, 2014). To measure fluorescence recovery after photobleaching, a solid-state 473 nm laser (MBL-FN-473-50mW, Dragon Laser) was coupled to the microscope light path using the photoactivation port on the microscope body. The laser beam was focused on the sample by the objective through an ET-GFP filter cube. A selected kinetochore cluster was manually aligned in the laser focus and exposed to the laser light for 100 ms. A 5-plane Z-stack (300 nm separation between adjacent planes) was acquired immediately before and after photobleaching, and then every 15 s for a total of 3 min. Maximum intensity projection of the Z-stack was used for fluorescence quantitation. The fluorescence of the photobleached kinetochore cluster (in a 6 × 6 pixel region around the brightest pixel) pre- and postbleach was measured, as was that of the region for each time point after photobleaching. Background fluorescence was subtracted from that of the region and a recovery graph was made using the fractional intensity at each time point relative to the pre-bleach signal. The methods used for image analysis have been described previously (Aravamudhan *et al.*, 2014).

Quantitative analysis of the spatial distribution of Stu2 and its mutant alleles

This analysis was conducted following the method developed previously (Sprague *et al.*, 2003). Briefly, a maximum-intensity projection image was generated from a stack of 10 Z planes separated by 200 nm for each cell. Next, the spindle axis defined by maximum-intensity pixels in the two spindle pole body spots was rotated so that it coincides with the horizontal axis. The cumulative intensity sum of a five-pixel-wide column centered on the spindle axis was calculated along the entire spindle axis and then normalized by the total fluorescence in the entire spindle. Finally, the normalized intensities were resampled to obtain 16 data points separated by 100 nm each (approximately equal to the pixel width of 107 nm) along the spindle axis.

Western blots

Yeast cells were grown at 30°C to mid–log phase in YPD. 3 OD_{600} cells were pelleted and lysed into Laemmli sample buffer (Bio-Rad 161-0737) by repeated vortexing with glass beads (Research Products International Corps #9831) and heating intermittently at 100°C. Total cell lysates were separated by electrophoresis on 10% SDS polyacrylamide gels and then transferred to nitrocellulose membranes. The blots were probed with mouse monoclonal antibodies against GFP (Clontech Living Colors A.v. monoclonal antibody [JL-8]; 1:5000) and mCherry (abcam Anti-mCherry antibody [1C51] ab125096; 1:2000), followed by peroxidase-conjugated anti-mouse immunoglobulin G (1:15,000; Sigma, A-4416). Blots were exposed to ECL reagent (Millipore Immobilon Western chemiluminescent HRP substrate, WBKLS0100), imaged with UVP ChemiDocIt Gel Imager using Vision Works LS Software or with the Azure Biosystem c600.

ACKNOWLEDGMENTS

This work was supported by R01-GM105948 from the National Institutes of Health to A.P.J. We thank Anthony Hyman, Luke Rice, and Tim Huffaker for sharing plasmids. We also thank Matt Miller and Sue Biggins for helpful discussions.

REFERENCES

Akiyoshi B, Sarangapani KK, Powers AF, Nelson CR, Reichow SL, Arellano-Santoyo H, Gonen T, Ranish JA, Asbury CL, Biggins S (2010). Tension directly stabilizes reconstituted kinetochore-microtubule attachments. Nature 468, 576–579.

Al-Bassam J, van Breugel M, Harrison SC, Hyman A (2006). Stu2p binds tubulin and undergoes an open-to-closed conformational change. J Cell Biol 172, 1009–1022.

Aoki K, Nakaseko Y, Kinoshita K, Goshima G, Yanagida M (2006). CDC2 phosphorylation of the fission yeast dis1 ensures accurate chromosome segregation. Curr Biol 16, 1627–1635.

Aravamudhan P, Felzer-Kim I, Gurunathan K, Joglekar AP (2014). Assembling the protein architecture of the budding yeast kinetochore–microtubule attachment using FRET. Curr Biol 24, 1437–1446.

Asbury CL, Gestaut DR, Powers AF, Franck AD, Davis TN (2006). The Dam1 kinetochore complex harnesses microtubule dynamics to produce force and movement. Proc Natl Acad Sci USA 103, 9873–9878.
Ayaz P, Munyoki S, Geyer EA, Piedra FA, Vu ES, Bromberg R, Otwinowski Z, Grishin NV, Brautigam CA, Rice LM (2014). A tethered delivery mechanism explains the catalytic action of a microtubule polymerase. Elife 3, e03069.
Ayaz P, Ye X, Huddleston P, Brautigam CA, Rice LM (2012). A TOG:alphabeta-tubulin complex structure reveals conformation-based mechanisms for a microtubule polymerase. Science 337, 857–860.
Bakhoum SF, Genovese G, Compton DA (2009). Deviant kinetochore microtubule dynamics underlie chromosomal instability. Curr Biol 19, 1937–1942.
Brouhard GJ, Stear JH, Noetzel TL, Al-Bassam J, Kinoshita K, Harrison SC, Howard J, Hyman AA (2008). XMAP215 is a processive microtubule polymerase. Cell 132, 79–88.
Driver JW, Geyer EA, Bailey ME, Rice LM, Asbury CL (2017). Direct measurement of conformational strain energy in protofilaments curling outward from disassembling microtubule tips. Elife 6, e28433.
Franck AD, Powers AF, Gestaut DR, Gonen T, Davis TN, Asbury CL (2007). Tension applied through the Dam1 complex promotes microtubule elongation providing a direct mechanism for length control in mitosis. Nat Cell Biol 9, 832–837.
Gandhi SR, Gierliński M, Mino A, Tanaka K, Kitamura E, Clayton L, Tanaka TU (2011). Kinetochore-dependent microtubule rescue ensures their efficient and sustained interactions in early mitosis. Dev Cell 21, 920–933.
Grishchuk EL, Efremov AK, Volkov VA, Spiridonov IS, Gudimchuk N, Westermann S, Drubin D, Barnes G, McIntosh JR, Ataullakhanov FI (2008). The Dam1 ring binds microtubules strongly enough to be a processive as well as energy-efficient coupler for chromosome motion. Proc Natl Acad Sci USA 105, 15423–15428.
Haruki H, Nishikawa J, Laemmli UK (2008). The anchor-away technique: rapid, conditional establishment of yeast mutant phenotypes. Mol Cell 31, 925–932.
He X, Rines DR, Espelin CW, Sorger PK (2001). Molecular analysis of kinetochore–microtubule attachment in budding yeast. Cell 106, 195–206.
Joglekar AP, Bouck DC, Molk JN, Bloom KS, Salmon ED (2006). Molecular architecture of a kinetochore–microtubule attachment site. Nat Cell Biol 8, 581–585.
Kim JO, Zelter A, Umbreit NT, Bollozos A, Riffle M, Johnson R, MacCoss MJ, Asbury CL, Davis TN (2017). The Ndc80 complex bridges two Dam1 complex rings. Elife 6, e21069.
Kosco KA, Pearson CG, Maddox PS, Wang PJ, Adams IR, Salmon ED, Bloom K, Huffaker TC (2001). Control of microtubule dynamics by Stu2p is essential for spindle orientation and metaphase chromosome alignment in yeast. Mol Biol Cell 12, 2870–2880.
Lampert F, Hornung P, Westermann S (2010). The Dam1 complex confers microtubule plus end-tracking activity to the Ndc80 kinetochore complex. J Cell Biol 189, 641–649.
Lampert F, Mieck C, Alushin GM, Nogales E, Westermann S (2013). Molecular requirements for the formation of a kinetochore–microtubule interface by Dam1 and Ndc80 complexes. J Cell Biol 200, 21–30.
Longtine MS, McKenzie A 3rd, Demarini DJ, Shah NG, Wach A, Brachat A, Philippsen P, Pringle JR (1998). Additional modules for versatile and economical PCR-based gene deletion and modification in *Saccharomyces cerevisiae*. Yeast 14, 953–961.
Maddox PS, Bloom KS, Salmon ED (2000). The polarity and dynamics of microtubule assembly in the budding yeast *Saccharomyces cerevisiae*. Nat Cell Biol 2, 36–41.
Malvezzi F, Westermann S (2014). "Uno, nessuno e centomila": the different faces of the budding yeast kinetochore. Chromosoma 123, 447–457.
Maurer SP, Cade NI, Bohner G, Gustafsson N, Boutant E, Surrey T (2014). EB1 accelerates two conformational transitions important for microtubule maturation and dynamics. Curr Biol 24, 372–384.
McIntosh JR, O'Toole E, Zhudenkov K, Morphew M, Schwartz C, Ataullakhanov FI, Grishchuk EL (2013). Conserved and divergent features of kinetochores and spindle microtubule ends from five species. J Cell Biol 200, 459–474.
Miller MP, Asbury CL, Biggins S (2016). A TOG protein confers tension sensitivity to kinetochore–microtubule attachments. Cell 165, 1428–1439.
Pearson CG, Maddox PS, Zarzar TR, Salmon ED, Bloom K (2003). Yeast kinetochores do not stabilize Stu2p-dependent spindle microtubule dynamics. Mol Biol Cell 14, 4181–4195.
Podolski M, Mahamdeh M, Howard J (2014). Stu2, the budding yeast XMAP215/Dis1 homolog, promotes assembly of yeast microtubules by increasing growth rate and decreasing catastrophe frequency. J Biol Chem 289, 28087–28093.
Powers AF, Franck AD, Gestaut DR, Cooper J, Gracyzk B, Wei RR, Wordeman L, Davis TN, Asbury CL (2009). The Ndc80 kinetochore complex forms load-bearing attachments to dynamic microtubule tips via biased diffusion. Cell 136, 865–875.
Severin F, Habermann B, Huffaker T, Hyman T (2001). Stu2 promotes mitotic spindle elongation in anaphase. J Cell Biol 153, 435–442.
Sprague BL, Pearson CG, Maddox PS, Bloom KS, Salmon ED, Odde DJ (2003). Mechanisms of microtubule-based kinetochore positioning in the yeast metaphase spindle. Biophys J 84, 3529–3546.
Tanaka K, Kitamura E, Kitamura Y, Tanaka TU (2007). Molecular mechanisms of microtubule-dependent kinetochore transport toward spindle poles. J Cell Biol 178, 269–281.
Tanaka TU (2010). Kinetochore–microtubule interactions: steps towards bi-orientation. EMBO J 29, 4070–4082.
Tien JF, Umbreit NT, Gestaut DR, Franck AD, Cooper J, Wordeman L, Gonen T, Asbury CL, Davis TN (2010). Cooperation of the Dam1 and Ndc80 kinetochore complexes enhances microtubule coupling and is regulated by aurora B. J Cell Biol 189, 713–723.
Umbreit NT, Miller MP, Tien JF, Ortola JC, Gui L, Lee KK, Biggins S, Asbury CL, Davis TN (2014). Kinetochores require oligomerization of Dam1 complex to maintain microtubule attachments against tension and promote biorientation. Nat Commun 5, 4951.
van Breugel M, Drechsel D, Hyman A (2003). Stu2p, the budding yeast member of the conserved Dis1/XMAP215 family of microtubule-associated proteins is a plus end-binding microtubule destabilizer. J Cell Biol 161, 359–369.
Vasileva V, Gierlinski M, Yue Z, O'Reilly N, Kitamura E, Tanaka TU (2017). Molecular mechanisms facilitating the initial kinetochore encounter with spindle microtubules. J Cell Biol, doi:10.1083/jcb.201608122.
Volkov VA, Zaytsev AV, Gudimchuk N, Grissom PM, Gintsburg AL, Ataullakhanov FI, McIntosh JR, Grishchuk EL (2013). Long tethers provide high-force coupling of the Dam1 ring to shortening microtubules. Proc Natl Acad Sci USA 110, 7708–7713.
Widlund PO, Stear JH, Pozniakovsky A, Zanic M, Reber S, Brouhard GJ, Hyman AA, Howard J (2011). XMAP215 polymerase activity is built by combining multiple tubulin-binding TOG domains and a basic lattice-binding region. Proc Natl Acad Sci USA 108, 2741–2746.
Wolyniak MJ, Blake-Hodek K, Kosco K, Hwang E, You L, Huffaker TC (2006). The regulation of microtubule dynamics in *Saccharomyces cerevisiae* by three interacting plus-end tracking proteins. Mol Biol Cell 17, 2789–2798.